

NRC Publications Archive Archives des publications du CNRC

Comparison of snow pressure measurements and theoretical predictions

McClung, D. M.; Larsen, J. O.; Hansen, S. B.

This publication could be one of several versions: author's original, accepted manuscript or the publisher's version. / La version de cette publication peut être l'une des suivantes : la version prépublication de l'auteur, la version acceptée du manuscrit ou la version de l'éditeur.

For the publisher's version, please access the DOI link below. / Pour consulter la version de l'éditeur, utilisez le lien DOI ci-dessous.

Publisher's version / Version de l'éditeur:

<https://doi.org/10.1139/t84-028>

Canadian Geotechnical Journal, 21, 2, pp. 250-258, 1984-05

NRC Publications Archive Record / Notice des Archives des publications du CNRC :

<https://nrc-publications.canada.ca/eng/view/object/?id=1659c46a-6164-413b-8a98-510610447c11>

<https://publications-cnrc.canada.ca/fra/voir/objet/?id=1659c46a-6164-413b-8a98-510610447c11>

Access and use of this website and the material on it are subject to the Terms and Conditions set forth at

<https://nrc-publications.canada.ca/eng/copyright>

READ THESE TERMS AND CONDITIONS CAREFULLY BEFORE USING THIS WEBSITE.

L'accès à ce site Web et l'utilisation de son contenu sont assujettis aux conditions présentées dans le site

<https://publications-cnrc.canada.ca/fra/droits>

LISEZ CES CONDITIONS ATTENTIVEMENT AVANT D'UTILISER CE SITE WEB.

Questions? Contact the NRC Publications Archive team at

PublicationsArchive-ArchivesPublications@nrc-cnrc.gc.ca. If you wish to email the authors directly, please see the first page of the publication for their contact information.

Vous avez des questions? Nous pouvons vous aider. Pour communiquer directement avec un auteur, consultez la première page de la revue dans laquelle son article a été publié afin de trouver ses coordonnées. Si vous n'arrivez pas à les repérer, communiquez avec nous à PublicationsArchive-ArchivesPublications@nrc-cnrc.gc.ca.

Ser
TH1
N21d

11288

no. 1175
c. 2
BLDG



National Research
Council Canada

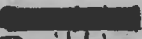
Conseil national
de recherches Canada

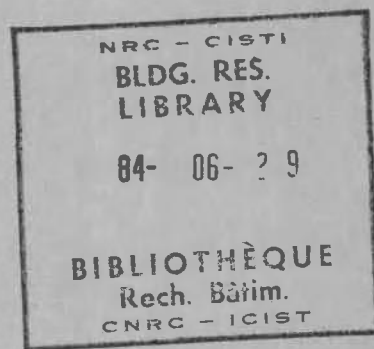
COMPARISON OF SNOW PRESSURE MEASUREMENTS AND THEORETICAL PREDICTIONS

by D. M. McClung, J. O. Larsen, and S. B. Hansen

ANALYZED

Reprinted from
Canadian Geotechnical Journal
Vol. 21, No. 2, May 1984
p. 250-258

DBR Paper No. 1175
Division of  Research
Building



This paper, while being distributed in reprint form by the Division of Building Research, remains the copyright of the original publisher. It should not be reproduced in whole or in part without the permission of the publisher.

A list of all publications available from the Division may be obtained by writing to the Publications Section, Division of Building Research, National Research Council of Canada, Ottawa, Ontario, K1A 0R6.

CISTI / ICIST



3 1809 00210 3486

Comparison of snow pressure measurements and theoretical predictions

DAVID M. MCCLUNG

National Research Council Canada, 3904 West 4th Avenue, Vancouver, B.C., Canada V6R 1P5

AND

JAN OTTO LARSEN AND SVEIN BORG HANSEN

Norges Geotekniske Institutt, Postboks 40 Taasen, Oslo 8, Norway

Received August 15, 1983

Accepted December 22, 1983

Measurements of snow creep pressures from the centre section of a 3.4 m high and 15 m long avalanche-defence supporting structure located on a mountain in western Norway are presented. The site has a deep snow cover and an average slope angle of 25°. The measurement configuration corresponds to plane-strain conditions and the data, along with measured snowpack parameters, allow comparison with simple theoretical predictions. The analysis shows that the average pressure on the structure may be calculated fairly accurately using linear, viscous modelling for the snow deformation. The maximum pressures proved to be higher than that provided by a linear model and this is considered characteristic of nonlinear material. The implications of these results for estimates of design loads are discussed.

Keywords: snow pressure, creep, measurements, viscous, plane-strain, finite element.

L'article présente des mesures de pression de fluage de la neige sur la section centrale d'une structure de protection contre les avalanches de 3,4 m de haut et 15 m de long, située sur une montagne dans l'ouest de la Norvège. Le site présente un couvert de neige épais et une pente moyenne de 25°. La configuration de l'installation de mesure correspond à des conditions de déformation plane et les données, associées aux paramètres mesurés du couvert de neige, permettent une comparaison avec des prédictions théoriques simples. L'analyse montre que la pression moyenne sur la structure peut être calculée avec une précision acceptable au moyen d'un modèle visqueux linéaire des déformations de la neige. Les pressions maximum se sont avérées plus fortes que celles déduites d'un modèle linéaire, ce qui est considéré typique d'un matériau non-linéaire. Les implications de ces résultats sur l'évaluation des charges de calcul sont discutées.

Mots-clés: pression de neige, fluage, mesure, viscosité, déformation plane, éléments finis.

[Traduit par la revue]

Can. Geotech. J. 21, 250-258 (1984)

Introduction

An important engineering problem concerning the design of structures on mountains with deep snow cover is the calculation of expected pressures due to interruption of snow creep (internal deformation) by the structure.

The simplest problem in relation to snow creep pressures is prediction of pressures at the centre of a long avalanche-defence supporting structure. This problem is of long-standing interest in snow mechanics; it was originally posed in the doctoral thesis of R. Haefeli (Bader *et al.* 1939). It is also the only creep pressure configuration for which serious analytic solutions have been proposed to date. These solutions are used extensively to aid in design considerations for structures.

In this study, creep pressures measured on the centre section of an avalanche-defence supporting structure are presented. The measurement site is in western Norway (altitude 1170 m) on a mountain with a deep snow cover on a nearly constant incline (average angle 25°). This configuration eliminates edge effects near the lateral ends of the structure, where fully three-dimensional modelling may be required, and it produces plane-strain measurement conditions.

The analytic models to date assume that snow behaves as a linear, Newtonian viscous fluid. This is obviously not a realistic assumption. It is of interest, however, to

compare the field measurements with these models. This comparison has two important motivating aspects: (1) by comparing actual measurements with a linear, viscous deformation model, those features of the problem that deserve attention for future, more realistic constitutive equations can be pinpointed; and (2) it would be very convenient for applications if a linear deformation model should prove useable for estimating the expected pressures, because of the simplicity of the solutions.

In the present paper field data are compared with the existing models of Haefeli (1948) and McClung (1982, 1984), and rigorous two-dimensional finite element calculations of the linear problem are provided as a check. The analysis indicates features of the linear problem worth retaining in a predictive scheme and illuminates some features of the data that disagree with the linear deformation model.

Experimental methods

Since the experimental methods for obtaining the pressures are discussed in detail in another paper,¹ only a short summary of the procedures is included here. Two

¹J. O. Larsen, M. D. McClung, and S. B. Hansen. The temporal and spatial variation of snow pressure on structures; in preparation.

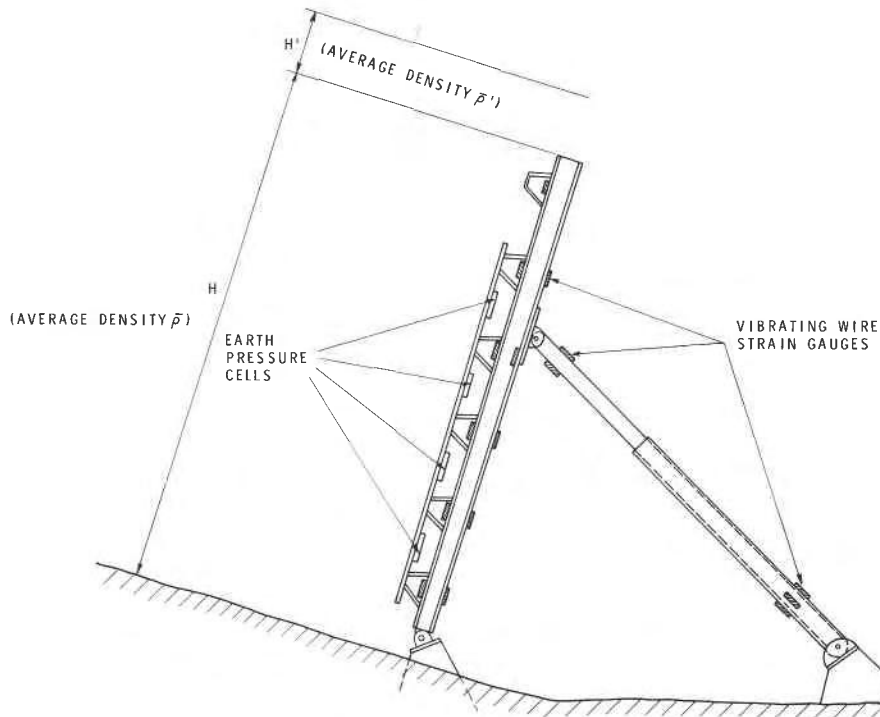


FIG. 1. Measurement site and location of strain gauges on structure. Primed variables denote quantities above the structure ($\bar{\rho}'$, H'); unprimed variables refer to quantities below the top of the structure ($\bar{\rho}$, H).

methods were employed: (1) direct measurement using laboratory-calibrated earth pressure cells mounted on the central portion of the structure; and (2) measurement of strains in the steel beams of the structure using vibrating wire strain gauges. These strains are subsequently used to deduce moment, shear, and pressure diagrams that describe the pressure dependence with depth on the structure.

Results have consistently shown that the earth pressure cell measurements are in fairly good agreement with the estimates derived from the strain-gauge data, provided the snowpack is dry. However, the earth pressure cell data are highly unreliable when the snowpack is wet. Thus, the pressure cell data are regarded as a check on the second measurement method when the snowpack is dry.

The second measurement method is used for the analysis in the present paper, since the results appear to be consistently reliable. Figure 1 is a schematic of the experimental setup, showing the location of the strain gauges on the structure. Because the structure is very rigid, the results lose accuracy when the product $\bar{\rho}gH$ is much less than 5 kPa ($\bar{\rho}$ is average snowpack density, g acceleration due to gravity, and H snowpack depth perpendicular to the ground surface). For values of $\bar{\rho}gH$ at 5 kPa and above, the average pressure can be estimated with less than 10% error; there is definitely more error for estimates of maximum pressure because

the pressure distribution cannot be determined uniquely. The rigidity of the system invalidates most of the early-season data, when the snowpack is shallow. This resulted in the loss of data for three winters when the snow cover was shallow.

Figure 2 gives an example of the pressure distribution with depth constructed from measured strains in the steel beams of the structure. Ideally, the average of two such diagrams, one from each of the main supports of the structure, should be used. However, because of harsh operating conditions, some gauges do not operate for a portion of the winter so that sufficient data are usually available for only one pressure diagram. The pressure does not go to zero at the top of the structure in Fig. 2 because the snowpack exceeds the structure height. The maximum pressure, σ_m , and the average pressure, $\bar{\sigma}$, are identified in Fig. 2.

To compare the measured pressures with simple theoretical models, the following properties of the snowpack were measured: density, temperature, and rammsonde hardness profiles, layering, and crystal types. Estimates were made of the free water content through the depth of the snowpack. These observations were made at least monthly, and sometimes more frequently, throughout the measuring period (Dec.–May) for the winters of 1975–1976, 1978–1979, 1980–1981, and 1981–1982). Glide shoes were placed on the rock surface uphill from the structure and it was verified that

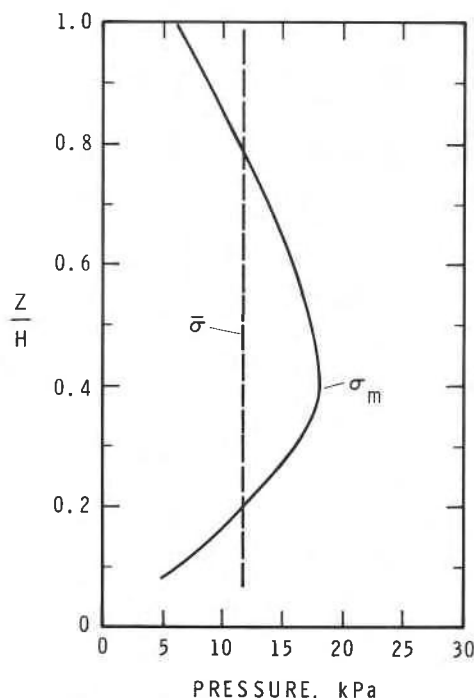


FIG. 2. Typical pressure distribution (—) on the structure versus relative height (z/H), where $z = 0$ represents the snow/ground interface. Constructed from strains measured in the steel beams of the structure for this example from 81-05-11. (σ_m) maximum pressure; $\bar{\sigma}$ (---) average pressure.

there was essentially no slip of the snow cover over the ground at the site.

Results and theoretical models

The measurements from the four winters are listed in Table 1, where $\bar{\rho}$ is the average snowpack density and H is the snow depth measured perpendicular to the ground surface (snowpack depth lower than or level with the top of the structure (3.4 m)). For portions of the snowpack higher than the structure, the average density is $\bar{\rho}'$ and the height for the snow above the structure is H' (see also Fig. 1). The snow depth values in Table 1 are average values measured upslope from the structure within its zone of influence for creep processes predicted by simple theory (McClung 1982). The densities were taken from snow pits near the site. Analysis of the data from Table 1 in relation to measured values of temperature and hardness from the snow profiles is given in Larsen *et al.*¹

It is necessary to modify the previously derived snow pressure equations to account for extra body forces when the snowpack depth exceeds the structure height. This may be accomplished by modifying the free surface boundary conditions that are appropriate when the snow depth is precisely equal to or less than the structure height. For the case of free surface boundary conditions

at the top of the snowpack, following McClung (1982, 1984), the average creep pressure on the face of a structure perpendicular to the ground on a slope with average angle ψ is given by

$$[1] \quad \frac{\bar{\sigma}}{\bar{\rho}gH} = \sin \psi \left[\left(\frac{2}{1-\nu} \right) \left(\frac{L}{H} \right) \right]^{1/2} + \frac{\cos \psi}{2} \left(\frac{\nu}{1-\nu} \right)$$

where ν is the viscous analog of Poisson's ratio for the assumed constitutive equation, which is a Newtonian viscous fluid with neglect of the static fluid pressure term. For [1], L/H is given by an empirical equation derived from numerical calculations (McClung 1984), and it is assumed that there is no glide. The expression for L/H is given as

$$[2] \quad \frac{L}{H} = 0.3[2 \cot \psi]^{1/2} \left(\frac{1-\nu}{1-2\nu} \right)^{1/4}$$

When the snowpack exceeds the height of the structure by H' and the average density above the structure is $\bar{\rho}'$ (Fig. 1), the free surface boundary conditions may be replaced by imposing initial shear and normal stresses on the surface level with the top of the structure. The new shear and normal boundary condition stresses are given by $\bar{\rho}'gH' \sin \psi$ and $\bar{\rho}'gH' \cos \psi$, respectively. By repeating the derivation given by McClung (1982), [1] may be modified to give

$$[3] \quad \frac{\bar{\sigma}}{(\bar{\rho}H + \bar{\rho}'H')(g)} \approx \sin \psi \left[\left(\frac{2}{1-\nu} \right) \left(\frac{L}{H} \right) \right]^{1/2} + \frac{\cos \psi}{2} \left[1 + \frac{1}{1 + \frac{\bar{\rho}H}{\bar{\rho}'H'}} \right] \left(\frac{\nu}{1-\nu} \right)$$

For a simple comparison with the theory, it is convenient to approximate the expression in brackets in the second term as

$$\left[1 + \frac{1}{1 + \frac{\bar{\rho}H}{\bar{\rho}'H'}} \right] \approx 1$$

so that [3] becomes

$$[4] \quad \frac{\bar{\sigma}}{(\bar{\rho}H + \bar{\rho}'H')(g)} \approx \sin \psi \left[\left(\frac{2}{1-\nu} \right) \left(\frac{L}{H} \right) \right]^{1/2} + \frac{\cos \psi}{2} \left(\frac{\nu}{1-\nu} \right)$$

The advantage of this approximation is that for terrain of constant incline ψ , the stress ratio is a function of ν only. Calculation with the data from Table 1 shows that the *maximum* error introduced by use of [4] instead of [3] would be less than 7% in the worst case (76-04-14) with ν taken as 0.4, which is considered an upper limit.

TABLE 1. Measured values of average and maximum pressure and related snowpack data

Date	Average pressure, $\bar{\sigma}$ (kPa)	Maximum pressure, σ_m (kPa)	Stress up to top of structure, $\bar{\rho}gH$ (kPa)	Excess stress over top of structure, $\bar{\rho}'gH'$ (kPa)	Total snow depth, $H + H'$ (m)
76-01-21	9	17	13.6	0.5	4.1
76-02-29	10	19	14.3	0.3	4.3
76-03-10	13	20	14.2	2.3	4.3
76-04-14	16	23	15.0	5.0	4.9
76-04-30	17	24	—	—	—
76-05-18	13	20	17.0	1.2	3.7
79-01-25	6	8	8.3	0.0	2.3
79-02-20	6	9	8.0	0.0	2.4
79-03-01	7	10	8.7	0.0	2.4
79-03-26	8	11	9.6	0.0	2.5
79-04-15	8	11	9.4	0.0	2.5
79-04-27	8	11	9.9	0.0	2.5
81-01-23	5	9	11.5	0.0	3.1
81-02-06	7	11	12.0	0.0	3.2
81-02-19	9	14	—	—	—
81-03-01	11	17	13.0	0.0	3.2
81-03-27	11	19	14.3	0.0	3.4
81-04-07	11	17	14.3	0.0	3.4
81-04-17	11	19	14.4	0.0	3.4
81-04-27	12	18	—	—	—
81-05-04	13	20	14.5	2.7	4.1
81-05-11	12	18	15.7	0.4	3.5
82-02-17	4	7	5.9	0.0	1.8
82-03-05	4	7	7.0	0.0	2.1
82-03-25	4	7	6.2	0.0	1.7
82-04-07	6	8	7.2	0.0	2.1
82-04-14	6	8	7.3	0.0	2.2
82-05-09	6	9	8.9	0.0	2.3

The *maximum* error for (76-03-10) and (81-05-04) would be about 4% and for all the other data points the maximum error would be negligible.

Haefeli's (1948) model gives the average creep pressure similar to [1] as

$$[5] \quad \frac{\bar{\sigma}}{\bar{\rho}gH} = \frac{2}{3} \left(\frac{1-\nu}{1-2\nu} \right)^{1/2} \tan \psi + \frac{\cos \psi}{2} \left(\frac{\nu}{1-\nu} \right)$$

By the same procedure, Haefeli's model is modified to account for nonfree surface conditions at the top of the structure:

$$[6] \quad \frac{\bar{\sigma}}{(\bar{\rho}H + \bar{\rho}'H')(g)} = \frac{2}{3} \tan \psi \left(\frac{1-\nu}{1-2\nu} \right)^{1/2} + \frac{\cos \psi}{2} \left(\frac{\nu}{1-\nu} \right)$$

for cases in which the snow depth exceeds the structure height.

Equations [4] and [6] do not account for extra shear

forces due to edge effects at the top of the structure when the snowpack is higher than the structure (Fig. 2). This consideration will be more important than the nonfree surface effects introduced in these equations in some instances. It implies that the estimates of average pressure will be slightly low for these conditions.

Comparison with theoretical predictions

Given the measurement site with a slope of nearly constant incline, the only free parameter in [4] and [6] is ν . This is also true for the full two-dimensional plane-strain solutions.

Clearly an important consideration for evaluation of the modelling is the range of expected values of ν in the density range of the experiments ($300 \text{ kg/m}^3 \leq \bar{\rho} \leq 550 \text{ kg/m}^3$). Salm (1977) has carefully reviewed the data and theoretical predictions; a summary of his work is as follows: Bader *et al.* (1951) provided an extensive range of laboratory estimates and they found values in the range $0.09 \leq \nu \leq 0.33$ for densities from 200 to 550 kg/m^3 . Pressure-at-rest field measurements by de

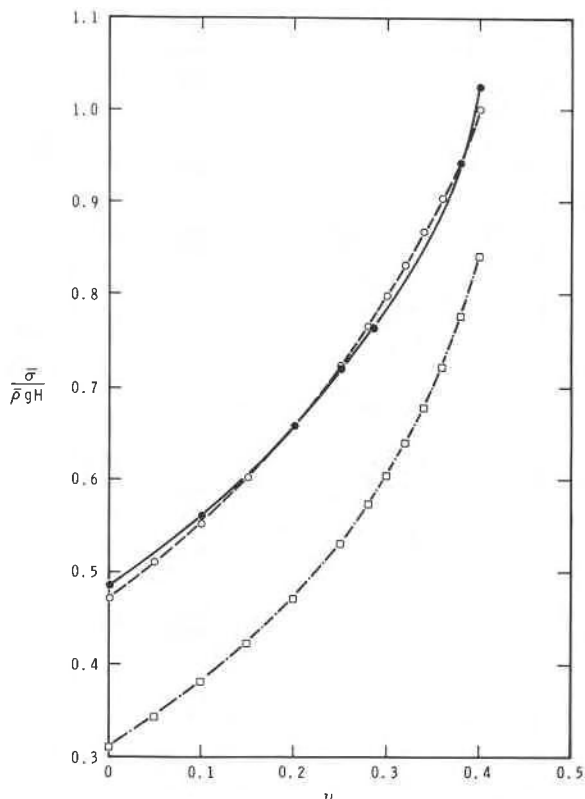


FIG. 3. Stress ratio $\bar{\sigma}/(\bar{\rho}gH)$ versus ν for the range $0 \leq \nu \leq 0.4$ for $\psi = 25^\circ$. Predictions shown are: (●—●) finite element calculations; (○---○) one-dimensional model with empirical corrections; (◇---◇) Haefeli's model.

Quervain (1966) and E. Klaussegger (unpublished data), quoted by Salm, indicate values in the range $0.08 \leq \nu \leq 0.35$ for this same density range. Haefeli (1966) provided creep angles for alpine snowpacks from which ν may be extracted. These values are $0.16 \leq \nu \leq 0.30$ for $\bar{\rho}$ between 350 and 550 kg/m^3 . McClung (1975) provided similar data, which indicate values between 0.23 and 0.38 , with an average value near 0.29 for final densities between 500 and 550 kg/m^3 .

Haefeli (1966) and Bader *et al.* (1951) also gave expressions for ν as a function of density based on theoretical arguments and their data. These predictions are $0.18 \leq \nu \leq 0.31$ and $0.13 \leq \nu \leq 0.22$ for $300 \text{ kg/m}^3 \leq \bar{\rho} \leq 500 \text{ kg/m}^3$.

With the above considerations, in order to ensure that the extreme limits of the data and theoretical predictions are included, the limits are taken as $0 \leq \nu \leq 0.4$. Figure 3 gives a comparison using [1], [2], and [5] for $\psi = 25^\circ$. Also shown in Fig. 3 are two-dimensional finite element predictions. The assumptions for all of these calculations are: no slip on the structure, no glide, a free surface at the snow/atmosphere interface and snow deforming as a linear, Newtonian viscous material with neglect of

the static fluid pressure term. The finite element calculations assume plane-strain conditions and these results give the 'dynamic' pressure due to interruption of creep deformation by the structure. In addition, a 'static' pressure term must be superimposed to represent the initial stresses in the formulation. This representation is analogous to the second terms on the right sides of [1] and [5] and is defined as

$$[7] \quad P_0(z) = \frac{\nu}{1-\nu} \int_0^{H-z} \rho \cos \psi \, dz' \\ \approx \frac{\nu}{1-\nu} \bar{\rho} g H \cos \psi \left(1 - \frac{z}{H}\right)$$

where z is measured perpendicular to the ground starting from $z = 0$ at the snow/earth interface. For the calculations given in Fig. 3, the maximum difference between the predictions of the model of McClung (1982, 1984) (given by [1] and [2]) and the finite element calculations is 2%. This agreement is fortuitous because deviations up to 6% have been found for other slope angles (McClung 1984).

For the data in Table 1, the stress ratio, $\bar{\sigma}/[(\bar{\rho}H + \bar{\rho}'H')(g)]$, has a mean of 0.73 and a standard deviation of 0.10 . This implies $\bar{\nu} = 0.25$ for the mean value for the predictions of the model given by [2] and [4] and it implies $\bar{\nu} = 0.36$ for Haefeli's model. The stress ratio spans a range of $0.44 \leq \bar{\sigma}/[(\bar{\rho}H + \bar{\rho}'H')(g)] \leq 0.85$, which implies a range of $-0.05 \leq \nu \leq 0.33$ for [2] and [4] and $0.16 \leq \nu \leq 0.40$ for Haefeli's model. Calculation of the implied value of ν for each data point from the measured stress ratio gives $\bar{\nu} = 0.25$ and a standard deviation of 0.09 for the average value of ν implied for [2] and [4]; it also gives $\bar{\nu} = 0.36$ and a standard deviation of 0.05 for Haefeli's model. If the lowest value of the stress ratio is discarded as a statistical outlier, the implied values of ν for the estimated values of the stress ratio are $0.11 \leq \nu \leq 0.33$ for [2] and [4], which is very close to the measured values for field and laboratory experiments in the density range. Figure 4 shows the comparison of measured values of $\bar{\sigma}$ versus $(\bar{\rho}H + \bar{\rho}'H')(g)$ and eqs. [2] and [4], finite element calculations, and Haefeli's model.

Of further interest with respect to the average pressure estimates are the results of the regression analysis reported by Larsen *et al.*¹ A regression analysis of the data in Table 1 showed that

$$[8] \quad \bar{\sigma} = 0.77(\bar{\rho}H + \bar{\rho}'H')(g) - 0.40 \text{ kPa}$$

with $r^2 = 0.89$ and the standard deviation of the residuals 1.1 kPa . This shows that $\bar{\sigma}$ is linear with $(\bar{\rho}H + \bar{\rho}'H')(g)$ to a good approximation, and the small intercept gives some added confidence in the data. The regression line is shown in Fig. 4. This analysis should not be extended beyond the current data set.

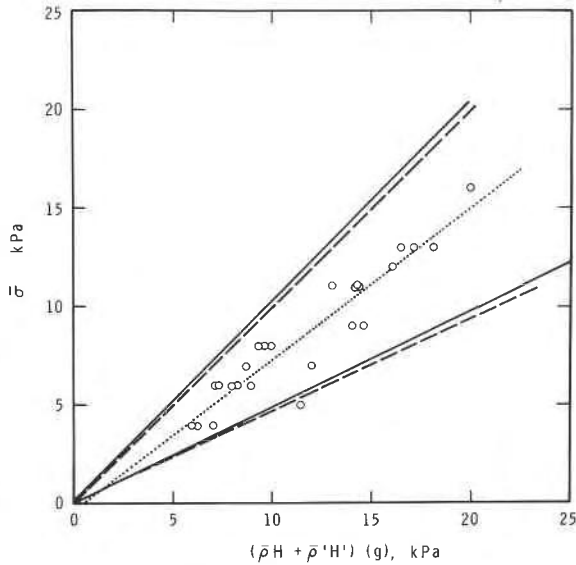


FIG. 4. Average pressure $\bar{\sigma}$ versus $(\bar{\rho}H + \bar{\rho}'H')(g)$ for data from Table 1. (○) estimates from field measurements; (---) predictions of one-dimensional model with empirical corrections; (—) finite element calculations. One-dimensional model and finite element calculations are shown for the limits $\nu = 0.0$ and $\nu = 0.4$. (···) regression line.

Data analyzed from similar measurements taken in Switzerland during the winters between 1950 and 1956 are presented in the Appendix. These data were taken on a slope with a near-constant incline of 37° (Salm 1977) and little or no glide. The Swiss data also indicate that $\bar{\sigma}$ is approximately linear with $(\bar{\rho}H + \bar{\rho}'H')(g)$ as is shown in the Appendix.

The one-dimensional models cannot be used to predict the maximum value, σ_m , of the pressure distribution. However, it is possible to calculate σ_m by finite element methods. Regression analysis of the data from Table 1 shows that σ_m is given by

$$[9] \quad \sigma_m = 1.25(\bar{\rho}H + \bar{\rho}'H')(g) - 1.25 \text{ kPa}$$

with $r^2 = 0.92$ and the standard deviation of the residuals 1.4 kPa (Larset *et al.*¹). The implication is that σ_m is linear with respect to $(\bar{\rho}H + \bar{\rho}'H')(g)$ to a good approximation. From Table 1, the mean value of the stress ratio $\sigma_m/[(\bar{\rho}H + \bar{\rho}'H')(g)]$ is 1.13, with a standard deviation of 0.13. Finite element calculations show that the ratio increases with ν , and has a value of 0.87 for $\nu = 0.25$ and 1.13 for $\nu = 0.40$. This result indicates that on the average the ratio exceeds predictions for linear modelling by about 30%, if $\bar{\nu} = 0.25$ is accepted as the mean value of ν from the results of the average pressure measurements.

Figure 5 depicts the relationship between σ_m and $\bar{\sigma}$ for the data as compared with finite element calculations. A

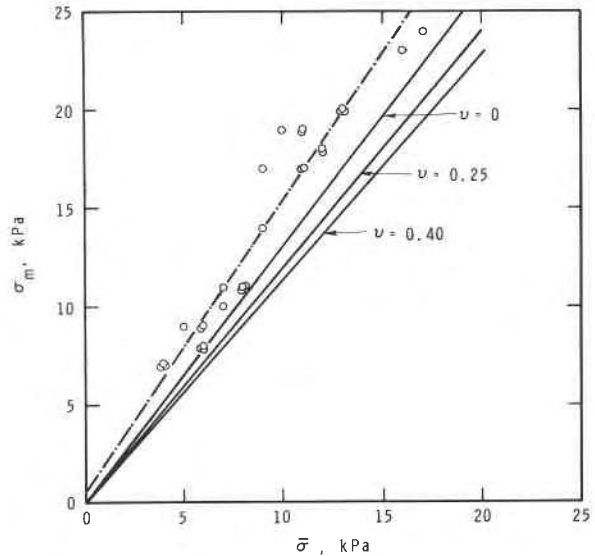


FIG. 5. Values of σ_m versus $\bar{\sigma}$ from the data and finite element calculations. (○) measured data points; (—) finite element calculations; (···) regression line.

regression analysis gives the result that

$$[10] \quad \sigma_m = 1.48\bar{\sigma} + 0.58 \text{ kPa}$$

with $r^2 = 0.93$ and the standard deviation of the residuals 1.4 kPa. Finite element calculations actually show that the stress ratio $\sigma_m/\bar{\sigma}$ declines as ν increases. From Table 1, the mean value of $\sigma_m/\bar{\sigma}$ is 1.55, with a standard deviation of 0.18. For $\bar{\nu} = 0.25$, which represents the average implied value of ν for the data if a linear viscous model is chosen, the finite element results give a value of $\sigma_m/\bar{\sigma} = 1.20$. The ratio thus exceeds the predictions for a linear material by about 30%.

Conclusions and discussion

From snow pressure measurements and analysis, the following conclusions have been reached.

1. The average pressure appears to be adequately explained by calculations assuming linear, viscous modelling. In this regard, the one-dimensional model of McClung (1982, 1984) with empirical corrections provides a formulation that agrees with field measurements as well as with finite element calculations.

2. The implied average value of ν is near 0.25 for the present measurements of $\bar{\sigma}$ when linear modelling is assumed. This is a reasonable value for alpine snow based upon experimental results in the density range of 300–500 kg/m³.

3. The maximum and the average pressures are linear with respect to $(\bar{\rho}H + \bar{\rho}'H')(g)$; the maximum pressure increases linearly with average pressure to a good approximation. The values of σ_m from field measure-

ments exceed predictions from linear modelling by about 30%.

4. Data from Switzerland analyzed in the Appendix give an implied average value of ν near 0.00, which is lower than measured values from other experiments for this density range. Regression analysis of the data from Switzerland shows that $\bar{\sigma}$ is approximately linear with $(\bar{\rho}H + \bar{\rho}'H')(g)$, in agreement with the data from the present study.

The implications of the results for maximum pressure must be accepted with caution because the accuracy is less than that for estimates of average pressure. If the results are accepted as valid in a qualitative sense, this feature of snow deformation implies nonlinear behaviour. Previous calculations by McClung (1976) showed that nonlinearity assumed by taking the effective shear and bulk viscosity proportional to the bulk stress provided relatively unchanged estimates of average pressure over a linear model, whereas the ratio $\sigma_m/\bar{\sigma}$ increased by about 15% for an example with $\psi = 45^\circ$. These nonlinear examples were complicated by glide but they seem to indicate qualitative agreement with the effects seen in the present data.

It was pointed out previously (McClung 1982) that the linear viscous model may be extended to the simplest viscoplastic model by making ν time dependent. It seems clear from Fig. 5 that this would not be sufficient to explain the present data. The finite element calculations in Fig. 5 show that the ratio $\sigma_m/\bar{\sigma}$ would decline as the snow densities and ν increase. The data in Fig. 5 seem to imply the opposite.

The most important result of this study with respect to applications is that the average pressure appears to be suitably described by the linear model. Since the one-dimensional model with empirical corrections provides a fairly accurate representation of the linear problem, a simple analytic method is available to predict average pressures. In addition, although the maximum pressure appears to exceed the predictions for a linear material, it may be accounted for in design by the usual engineering safety factors. The regression analysis for the data presented shows (eq. [10]) that σ_m is about $1\frac{1}{2}$ times the average pressure. The standard deviation of the residuals (1.4 kPa) used in connection with [9] would allow estimates of σ_m to any chosen confidence limit for the data presented. Study of more accurate nonlinear viscoplastic models for snow deformation that provide the descriptive features seen in the data may permit prediction of the maximum pressure from a better theoretical framework.

Acknowledgements

We wish to thank K. Kristensen, Norges Geotekniske Institutt (NGI), for his help in collection of the field data. We also wish to thank B. Schieldrop, Industriell

Hydro-og Aerodynamikk, Oslo, and K. Høeg, NGI, for many useful technical suggestions. Peter Schaerer, National Research Council Canada, read the first draft of this paper and provided many useful suggestions.

This work was partially funded by Norges Vassdrags-og Elektrisitetsvesen, Oslo, and we are grateful for their support.

This paper is a joint contribution from the Division of Building Research, National Research Council Canada and the Norwegian Geotechnical Institute and is published with the approval of the Directors of these institutions.

BADER, H., HAEFELI, R., BUCHER, E., NEHERER, J., ECKEL, O., THAMS, C., and NIGGLI, P. 1939. Der Schnee und seine Metamorphose, Beiträge zur Geologie der Schweiz. Geotechnische Serie, Hydrologie, Lief 3. (German, English translation, U.S. Snow, Ice and Permafrost Research Establishment, Trans. 14, 1954.)

BADER, H., HANSEN, B. L., JOSEPH, J. H., and SANDGREN, M. A. 1951. Preliminary investigations of some physical properties of snow. U.S. Snow, Ice and Permafrost Research Establishment. Report 7.

DE QUERVAIN, M. R. 1966. Measurements on the pressure at rest in a horizontal snow cover. Union de Géodésie et Géophysique Internationale. Association Internationale d'Hydrologie Scientifique. Commission pour la Neige et la Glace. Division Neige Saisonnière et Avalanches. Symposium Internationale sur les Aspects Scientifiques des Avalanches de Neige, 5–10 avril 1965, Davos, Suisse, pp. 154–159. (Publication N° 69 de l'Association Internationale d'Hydrologie Scientifique.)

HAEFELI, R. 1948. Schnee, Lawinen, Firm und Gletscher. In Ingenieur-Geologie. 2 Bd. Edited by L. Bendel. Springer-Verlag, Vienna, pp. 663–735.

——— 1966. Considerations sur la pente critique et le coefficient de pression au repos de la couverture de neige. Union de Géodésie et Géophysique Internationale. Association Internationale d'Hydrologie Scientifique. Commission pour la Neige et la Glace. Division Neige Saisonnière et Avalanches. Symposium Internationale sur les Aspects Scientifiques des Avalanches de Neige, 5–10 avril 1965, Davos, Suisse, pp. 141–153. (Publication N° 69 de l'Association Internationale d'Hydrologie Scientifique.)

KÜMMERLI, F. 1958. Auswertung der Druckmessungen am Druckapparat Institut (DAI). Interner Bericht des Eidg. Institutes für Schnee und Lawinenforschung, Nr. 240.

McCLUNG, D. M. 1975. Creep and the snow–earth interface condition in the seasonal alpine snowpack. (Union Géodésique et Géophysique Internationale. Association Internationale des Sciences Hydrologiques. Commission des Neiges et Glaces.) Symposium. Mécanique de la neige. Actes du colloque de Grindelwald, avril 1974, pp. 236–248. (IAHS-AISH Publication No. 114.)

——— 1976. Snowpressure on rigid obstacles. Journal of Glaciology, 17(76), pp. 277–285.

——— 1982. A one-dimensional analytical model for snow creep pressures on rigid structures. Canadian Geotechnical Journal, 19(4), pp. 401–412.

——— 1984. Empirical corrections to snow creep pressure

equations. Canadian Geotechnical Journal, **21**(1), pp. 191–193.

SALM, B. 1977. Snow forces. Journal of Glaciology, **19**(80), pp. 67–100.

Appendix

Data have been obtained from an observation site at the Weissflujoch (altitude 2680 m) in eastern Switzerland. The experiments have been described by Salm (1977) from the original report of Kümmerli (1958). The observation site has a configuration similar to that for the data reported from Norway. The slope angle is a nearly constant incline of 37° and measurements showed no glide upslope from the structure. The measurements were taken from the centre section of an avalanche-defence structure, where lateral edge effects would be largely absent. The average snowpack densities ranged from 220 to 520 kg/m³.

There are two potentially important differences in the data sets from Switzerland and Norway: (1) snowpack properties and (2) measurement techniques. Without further analysis, it is not possible to quantify the differences in snowpack structure between these two sites. Salm (1977) and Kümmerli (1958) have described how the loads were calculated from the deformation of springs on each of the horizontal crossbeams. Kümmerli (1958) lists data for the total force on the structure for six winters of observations. From these resultant forces, the average pressure on the structure has been calculated using [4] and [6]. Figure A1 shows the comparison of the predictions of finite element calculations and [1] and [5] over the range of interest: $0 \leq \nu \leq 0.4$ for $\psi = 37^\circ$ analogous to Fig. 3. In Fig. A2, the implied values of $\bar{\sigma}$ are plotted versus $(\bar{\rho}H + \bar{\rho}'H')(g)$, similar to the comparison in Fig. 4 for the Norwegian data. From Fig. A2, nearly half of the data points imply negative values of ν . For the 78 data points in Fig. A2, the average value of $\bar{\sigma}/[(\bar{\rho}H + \bar{\rho}'H')(g)]$ is 0.58, with a standard deviation of 0.12. This implies an average value of $\bar{\nu} = 0.0$ for the finite element calculations, $\bar{\nu} = -0.02$ for [4], and $\bar{\nu} = 0.10$ for Haefeli's model (eq. [6]). Figure A1 shows that Haefeli's model provides fairly accurate estimates of the linear problem for $\psi = 37^\circ$; this is fortuitous. The data imply a stress ratio in the range $0.34 \leq \bar{\sigma}/[(\bar{\rho}H + \bar{\rho}'H')(g)] \leq 0.86$. This yields $-0.50 \leq \nu \leq 0.26$ for the prediction of [4] and $-0.38 \leq \nu \leq 0.31$ for Haefeli's model.

A regression analysis was performed for the data depicted in Fig. A2. This analysis gave the relation $\bar{\sigma} = 0.69(\bar{\rho}H + \bar{\rho}'H')(g) - 1.05$ kPa with $r^2 = 0.82$ and standard deviation of the residuals 1.2 kPa. Power law regression gave $\bar{\sigma} = 0.36[(\bar{\rho}H + \bar{\rho}'H')(g)]^{1.20}$ with $r^2 = 0.84$ and the standard deviation of the residuals approximately 1.2 kPa.

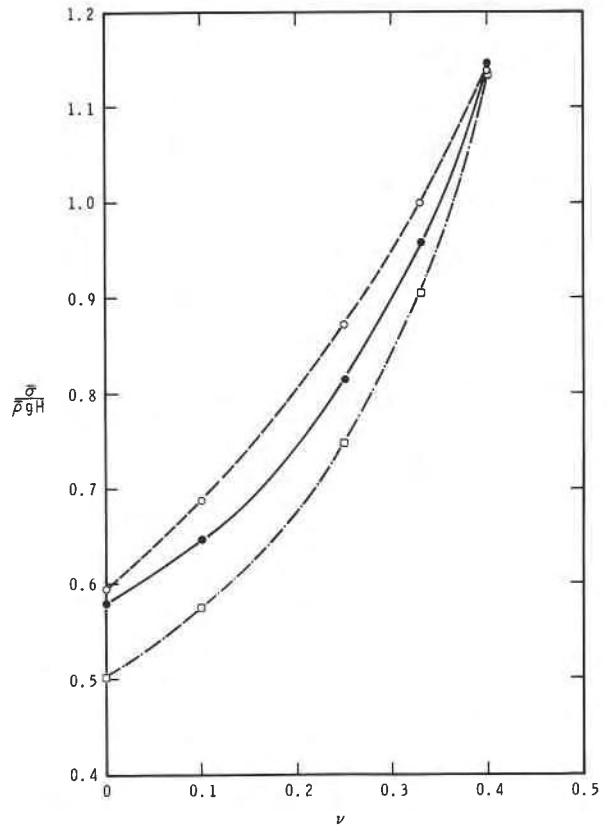


FIG. A1. Stress ratio $\bar{\sigma}/(\bar{\rho}gH)$ versus ν for the range $0 \leq \nu \leq 0.4$ for $\psi = 37^\circ$. Predictions shown are (●—●) finite element calculations; (○—○) one-dimensional model with empirical corrections; and (◇---◇) Haefeli's model.

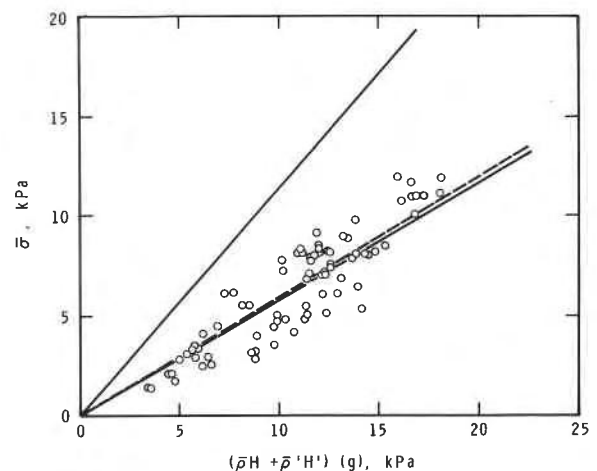


FIG. A2. Average pressure $\bar{\sigma}$ versus $(\bar{\rho}H + \bar{\rho}'H')(g)$ for data from Switzerland. (○) measurement points; (—) limits of finite element calculations; and (---) one-dimensional model for $\nu = 0.0$ and $\nu = 0.4$. These latter two predictions are identical for $\nu = 0.4$.

The following conclusions seem evident from this data analysis.

1. The implied values of ν and $\bar{\nu}$ are too low when compared with laboratory and field measurements for the density range in question. The measurements imply average pressures that are less than the value for a linear viscous material.

2. The regression analysis shows that $\bar{\sigma}$ is approximately linear with $(\bar{\rho}H + \bar{\rho}'H')(g)$. Although the power law regression analysis shows a slightly better fit, these results must be accepted with caution because the actual values of $\bar{\sigma}$ appear to be less than that implied by the linear constitutive equation.